Pure Appl. Chem., Vol. 84, No. 3, pp. 663–673, 2012.
http://dx.doi.org/10.1351/PAC-CON-11-06-01

Direct synthesis of dimethyl carbonate from methanol and carbon dioxide over organotin-functionalized mesoporous benzene-silica*

Binbin Fan[1], Hongyu Li[1], Weibin Fan[2,‡], Zhangfen Qin[2,‡], and Ruifeng Li[1,‡]

[1]Institute of Special Chemicals, Taiyuan University of Technology, 79 West Yingze Street, Taiyuan, Shanxi 030024, China; [2]State Key Laboratory of Coal Conversion, Institute of Coal Chemistry, Chinese Academy of Sciences, P.O. Box 165, Taiyuan, Shanxi 030001, China

Abstract: Ordered periodic mesoporous benzene-silicas (Ph-PMOs) functionalized with organotin were synthesized by co-condensing $(MeO)_2ClSi(CH_2)_3SnCl_3$, tetraethyl orthosilicate (TEOS), and 1,4-bis(triethoxysilyl)-benzene in a Pluronic 123 acid solution. The diffraction lines for (100), (110), and (200) facets observed in their X-ray diffraction (XRD) patterns and parallel channels in their transmission electron microscopy (TEM) images show that the samples have highly ordered hexagonal array structure. The presence of bands characteristic for phenyl groups, tetrahedral and octahedral Sn species, and Q^n and T^n species in their Fourier transform/infrared (FT/IR), diffuse reflectance UV–vis, and NMR spectra gives convincing evidence for the incorporation of phenyl groups and $(MeO)_2ClSi(CH_2)_3SnCl_3$ into the framework or silica wall. The organotin-functionalized Ph-PMOs exhibit much higher catalytic activity than organotin-functionalized mesoporous silica lacking phenyl groups in the framework, for direct synthesis of dimethyl carbonate (DMC) from methanol and CO_2, although both have high catalytic stability. This may be attributed to its enhanced surface hydrophobicity and the presence of a large number of hexa-coordinated Sn species and tiny Sn oxide clusters in the former sample. The DMC yield obtained over the prepared organotin-functionalized Ph-PMOs increases monotonically with increasing CO_2 pressure. The material also exhibits high catalytic stability upon reusage.

Keywords: carbon dioxide; dimethyl carbonate; methanol; organotin; periodic mesoporous organosilicas.

INTRODUCTION

Periodic mesoporous organosilicas (PMOs) synthesized by employing bridged silsesquioxanes as silica sources are highly ordered organic/inorganic hybridized mesoporous materials. Incorporation of organic groups into the framework not only alters the surface properties of mesoporous materials, but also introduces and/or facilitates modification of organic functionalities [1–3]. Up to now, PMOs with simple bridging groups derived from methane, ethane, ethylene, urea, benzene and its derivatives, thiophene, ferrocene, etc. have been synthesized [4–11]. PMOs as catalysts or supports have attracted much

Pure Appl. Chem.* **84, 411–860 (2012). A collection of invited papers for the IUPAC project 2008-016-1-300 "Chlorine-free Synthesis for Green Chemistry".

‡Corresponding authors: fanwb@sxicc.ac.cn (W. Fan); qzhf@sxicc.ac.cn (Z. Qin); rfli@tyut.edu.cn (R. Li)

attention due to their unique properties. However, most of the bridging organic groups are chemically inert and lack the necessary functionalities for applications in catalysis [12]. In this context, second groups carrying specific functions, such as transition-metal cations or clusters (Al, Ti, Cr, V, and Au), sulfonic acid, amine and chiral metal complexes, have been incorporated into the pore wall or encapsulated in the nanopores of PMOs [12–18]. The obtained materials generally show higher catalytic activity than the corresponding mesoporous silica counterparts owing to their improved surface hydrophobicity [12].

Dimethyl carbonate (DMC) is an environmentally benign chemical and displays versatile reactivity. These properties make DMC attractive as an eco-friendly alternative to both methyl halides (or dimethyl sulfate) and phosgene in methylation and carbonylation processes [19–21]. CO_2 is readily available, inexpensive, and nontoxic, but contributes toward inducing the greenhouse effect. Accordingly, direct synthesis of DMC from methanol and CO_2 has much to commend it as a green process. Nevertheless, this process is a challenge because of the chemical inertness of CO_2. Although organotin compounds such as dibutyl-dialkyoxystannanes can promote carbonation of alcohol [22], their high mammalian toxicity and homogeneous character limit large-scale application, owing to resultant disposal difficulties arising from their fugacity and lability toward hydrolysis, photodegradation, and biodegradation [23]. Therefore, heterogenization of organotins is desirable to facilitate catalyst separation, resultant recovery, and catalyst reuse. We have prepared a functional heterogeneous organotin catalyst of $(MeO)_2ClSi(CH_2)_3SnCl_3$ tethered on SBA-15 in situ, which shows high activity for the direct synthesis of DMC from methanol and carbon dioxide [24]. In this work, we report the synthesis of organotin-functionalized mesoporous benzene-silicas (Ph-PMOs) and their catalytic performance in the synthesis of DMC from methanol and CO_2.

EXPERIMENTAL

Preparation of organotin-functionalized Ph-PMOs

$(MeO)_2ClSi(CH_2)_3SnCl_3$ (**1**) was synthesized according to the method reported in ref. [24].

Organotin-functionalized Ph-PMOs were synthesized with tetraethyl orthosilicate (TEOS), Pluronic 123 (P123), hydrocholoric acid (HCl), distilled water, 1,4-bis(triethoxysilyl) benzene (BTEB), and **1** in terms of the composition of 12 HCl : 1 (*a* TEOS + *b* BTEB) : 0.085 (**1**) : 0.017 P123 : 600 H_2O (*b*/*a* = 0–4 mol/mol). In a typical batch, 4 g of P123 was first dissolved in 438 g of 1.1 M HCl aqueous solution at room temperature. To this solution required amounts of TEOS and BTEB were added. It was then heated to 40 °C and kept for 1 h under stirring. This was followed by slow addition of **1**. The resultant mixture was further agitated at 40 °C for 20 h and statically maintained at 80 °C for 6 h. The solid product was filtered, washed with deionized water, and dried at ambient temperature. The surfactant in the solid product was removed by extracting it in a 0.12 M HCl ethanolic solution for 48 h. The extracted sample was dried at room temperature, and then treated with methanolic triethylamine (TEA) (TEA/CH_3OH = 1/30 (mL/mL), liquid/solid = 15/1 (mL/g)) under reflux for 24 h. The resultant organotin-functionalized Ph-PMOs sample was washed with methanol five times and dried at room temperature under vacuum conditions.

Characterization of organotin-functionalized Ph-PMOs

Powder X-ray diffraction (XRD) patterns were recorded on a Rigaku D/Max-2500 diffractometer (40 kV, 40 mA) with Cu Kα radiation. High-resolution transmission electron microscopy (HRTEM) images were collected on a JEOL JEM-2010 microscope at an acceleration voltage of 120 kV.

N_2 adsorption/desorption measurements were carried out at –196 °C on a Quantachrone Nova 1200e physisorption analyzer. Before each measurement, the sample was evacuated at 200 °C for half an hour. Brunauer–Emmett–Teller (BET) surface area was calculated from adsorption branch in the

range of relative pressure from 0.05 to 0.25, while pore size was evaluated from desorption branch by the Barrett–Joyner–Halenda (BJH) method. Pore volume was estimated at a relative pressure of 0.99.

Diffuse reflectance UV–vis spectra of samples were measured on a Perkin-Elmer Lambda Bio40 UV–vis spectrophotometer equipped with an integration sphere. ^{29}Si and ^{13}C CP MAS NMR spectra of samples were recorded at 59.6 and 75.4 MHz, respectively, on a Varian Unity INOVA NMR spectrometer (300 MHz). Sn content in the prepared organotin-functionalized Ph-PMOs was determined by an inductively coupled plasma/atomic emission spectrometer (ICP/AES).

The adsorption isotherms of H_2O on these samples were measured on a BEL-max instrument (Bel Japan, Inc.) at 25 °C. Before each measurement, the sample was preheated at 110 °C for 6 h under high vacuum.

Catalytic tests

Direct synthesis of DMC from methanol and CO_2 was conducted in a 100-mL stainless steel batch reactor (Parr) equipped with a thermal couple, a magnetic stirrer, and a heater. Typical reaction conditions were as follows: 0.05 g of catalyst, 20 mL of methanol, CO_2 pressure of 18.0 MPa, reaction temperature of 180 °C, reaction time of 10 h. The product was analyzed with an Agilent GC 7890 gas chromatograph equipped with a 60-m SE-30 capillary column and a flame ionization detector.

RESULTS AND DISCUSSION

Characterization of organotin-functionalized Ph-PMOs

Table 1 gives the notations (Sn-Ph-PMOs-*x*, *x* representing the molar ratio of BTEB/TEOS), Sn contents, and physical properties of the extracted organotin-functionalized Ph-PMOs samples. The previous work showed that the optimum molar ratio of **1**/TEOS was 0.085 for synthesis of highly ordered organotin-functionalized SBA-15 with high activity in the synthesis of DMC from methanol and CO_2 [22,24]. Thus, the molar ratio of **1**/(TEOS + BTEB) was kept at 0.085 for synthesis of Sn-Ph-PMOs samples in this work. Figure 1 shows that the samples synthesized with the gels having different amounts of BTEB all exhibit three diffraction lines in the 2θ range of 0.5–4º in their XRD patterns, which are indexed to (100), (110), and (200) facets, indicative of highly ordered hexagonal array structures. This is further confirmed by the TEM images of Sn-Ph-PMOs-0.67 (Fig. 2), which as an example clearly reveal the well-defined hexagonally arranged porous channels. Nevertheless, the structural order of the as-synthesized samples degrades with increasing BTEB content in the synthesis gel. As a result, Sn-Ph-PMOs-4.0 shows only one diffraction line at 2θ of 0.9º. This is consistent with the lowered electron contrast between the walls and the channels of the silica network [25]. The incorporation of **1** and BTEB in the framework causes a severe structure distortion, and the distortion degree increases with the amounts of **1** and BTEB incorporated [24]. A similar phenomenon was observed for the sulfonic acid-functionalized PMOs synthesized by co-condensing tetramethoxysilane, 1,2-bis(trimethoxysilyl)-ethane, and 3-mercaptopropyltrimethoxysilane in acidic medium in the presence of P123 surfactant and inorganic salt additives [25].

Table 1 Chemical compositions and physical properties of Sn-Ph-PMOs-*x* samples.

Sample	BTEB/TEOS (mol/mol)	S_{BET} (m^2/g)	d_P (nm)	V_P (mL/g)	Sn/Si (mmol/mol)
Sn-Ph-PMOs-0	0	310	3.75	0.28	6.43
Sn-Ph-PMOs-0.25	0.25	424	3.43	0.31	5.00
Sn-Ph-PMOs-0.67	0.67	508	5.41	0.41	4.85
Sn-Ph-PMOs-4	4.00	519	4.32	0.47	4.69

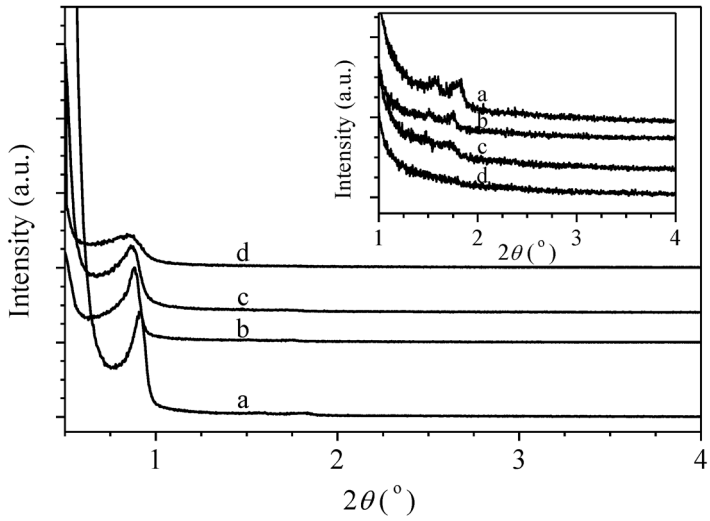

Fig. 1 XRD patterns of (a) Sn-Ph-PMOs-0, (b) Sn-Ph-PMOs-0.25, (c) Sn-Ph-PMOs-0.67, and (d) Sn-Ph-PMOs-4.0 (inserted graph, magnified XRD patterns).

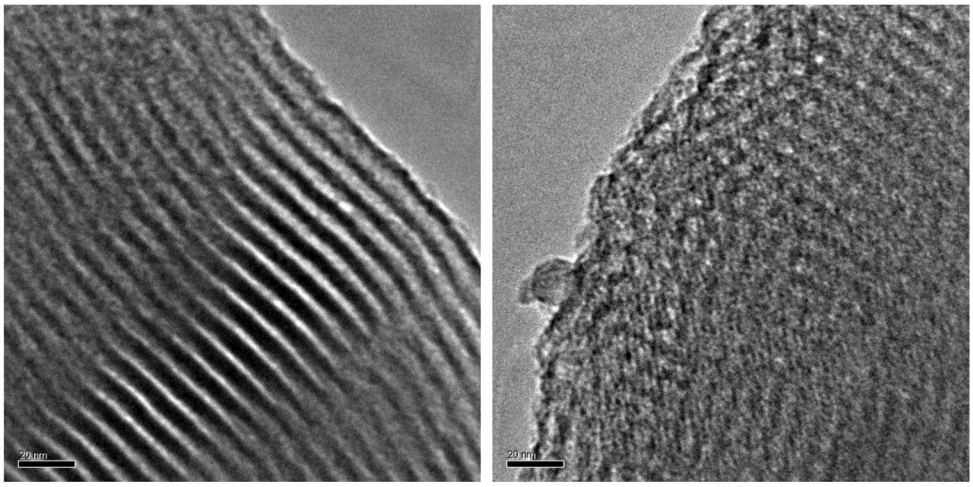

Fig. 2 TEM images of Sn-Ph-PMOs-0.67 sample along (a) (100) and (b) (110) incidences (scale bar: 20 nm).

Table 1 shows that the presence of BTEB in the synthesis gel leads to a decrease in the amount of incorporated **1**, as evidenced by the lower Sn content in Sn-Ph-PMOs-*x* ($x > 0$) than that in Sn-Ph-PMOs-0. This may be a result of the competitive insertion of BTEB with that of **1** in the framework. To synthesize highly ordered mesostructured material in the presence of both BTEB and **1**, the crystallization temperature was lowered and the crystallization time was shortened, which, however, resulted in an ineffective condensation of **1** with TEOS and BTEB but a tethering of it on the pore wall of the obtained mesoporous materials.

The N_2 adsoption/desorption isotherms of Sn-Ph-PMOs-*x* samples are shown in Fig. 3. A typical type IV profile with a H1 hysteresis loop is observed for all the samples, further demonstrating that the prepared materials possess a mesoporous structure. The BET surface area and the pore volume increase

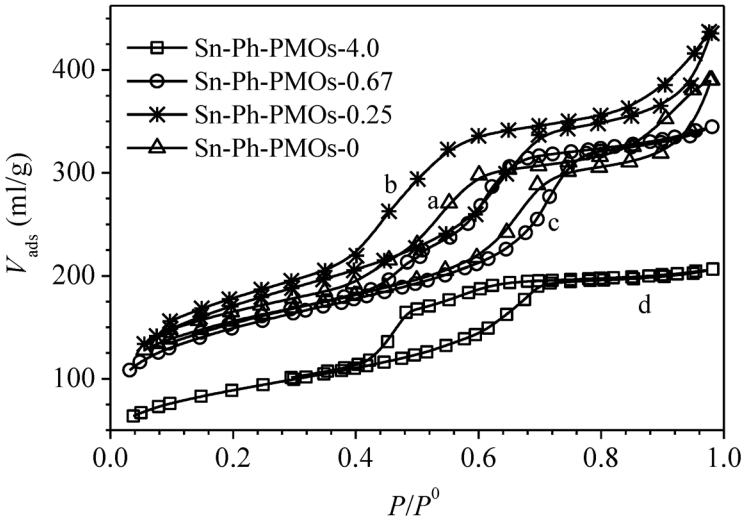

Fig. 3 N_2 adsorption/desorption isotherms of (a) Sn-Ph-PMOs-0, (b) Sn-Ph-PMOs-0.25, (c) Sn-Ph-PMOs-0.67, and (d) Sn-Ph-PMOs-4.0 at –196 °C.

with increasing BTEB content in the synthesis gel up to a BTEB/TEOS molar ratio of 0.67. The incorporation of more BTEB into the framework leads to an expansion of the unit cell, giving a larger void space. However, a further increase of the BTEB content in the synthesis gel results in a decrease of the BET surface area and the pore volume, as a result of the serious deterioration of the mesoporous structure. Although the average pore diameter is in the range of 3.5–5.5 nm, the pore size distribution is broadened for the sample synthesized with the gel having a BTEB/TEOS molar ratio higher than 0.67.

The diffuse reflectance UV–vis spectra of Sn-Ph-PMOs-*x* samples are displayed in Fig. 4. For Sn-Ph-PMOs-0, only one band is observed at 205 nm, which is attributed to tetrahedral Sn species [24], while another two bands around 220 and 269 nm ascribed to the phenyl groups are also present besides

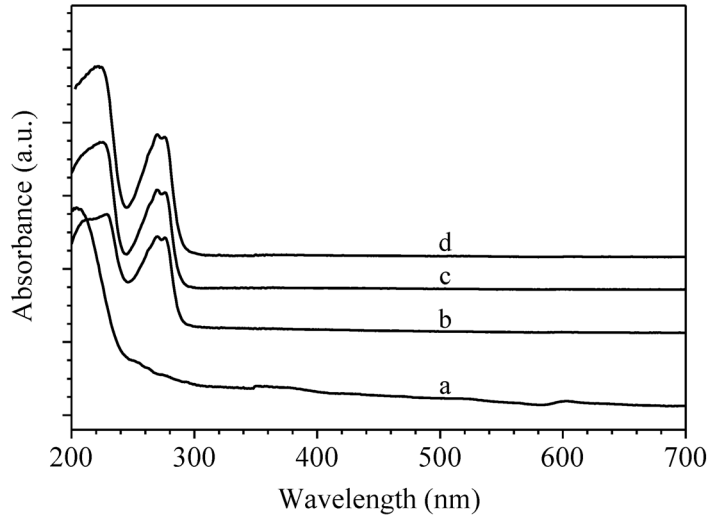

Fig. 4 DR UV–vis spectra of (a) Sn-Ph-PMOs-0, (b) Sn-Ph-PMOs-0.25, (c) Sn-Ph-PMOs-0.67, and (d) Sn-Ph-PMOs-4.0.

the band at 205 nm in the spectra of Sn-Ph-PMOs-*x*. The obvious decrease in the intensity of the 205-nm band with increasing BTEB amount suggests that more tetrahedral Sn species are transformed into octahedral Sn species or tiny Sn oxide clusters, although their characteristic bands are overlapped by the 269-nm band for the phenyl groups [26]. This indicates that the structure of **1** is kept intact during the synthesis process and that the organotin and phenyl moieties are simultaneously incorporated into and/or immobilized on the Sn-Ph-PMOs samples.

Figure 5 shows as an example the ^{13}C and ^{29}Si CP MAS NMR spectra of the Sn-Ph-PMOs-0.25 sample. The intense peak at 133 ppm in the ^{13}C CP MAS NMR spectrum (Fig. 5a) is attributed to the presence of benzene-bridging groups [27], while those at 17–30 ppm are ascribed to the propyl groups directly bonded to Si atoms [24]. This proves the non-cleavage of **1** during the synthesis and the simultaneous presence of organotin and benzene groups in the Sn-Ph-PMOs-*x* samples. The presence of a peak at about 45 ppm, assigned to C-SiOCH_3 group in **1** [28], indicates that the hydrolysis/condensation of **1** is not complete during the synthesis process. The nearly complete removal of the P123 surfactant is corroborated by the absence of peaks between 66 and 77 ppm. The ^{29}Si CP MAS NMR spectrum of Sn-Ph-PMOs-0.25, as expected, confirms that both $Si(OSi)_{1-n}(OH)_n$ and $Si(OSi)_{1-n}(OC)_n$ species exist in the sample (Fig. 5b). The characteristic resonance signals in the region from –120 to –90 ppm are assigned to Q^4 (–113 ppm), Q^3 (–103 ppm), and Q^2 (–95 ppm) species, while those centered at 81.5 and 79.1 ppm are attributed to T^3 species joint with phenyl groups and **1**, respectively

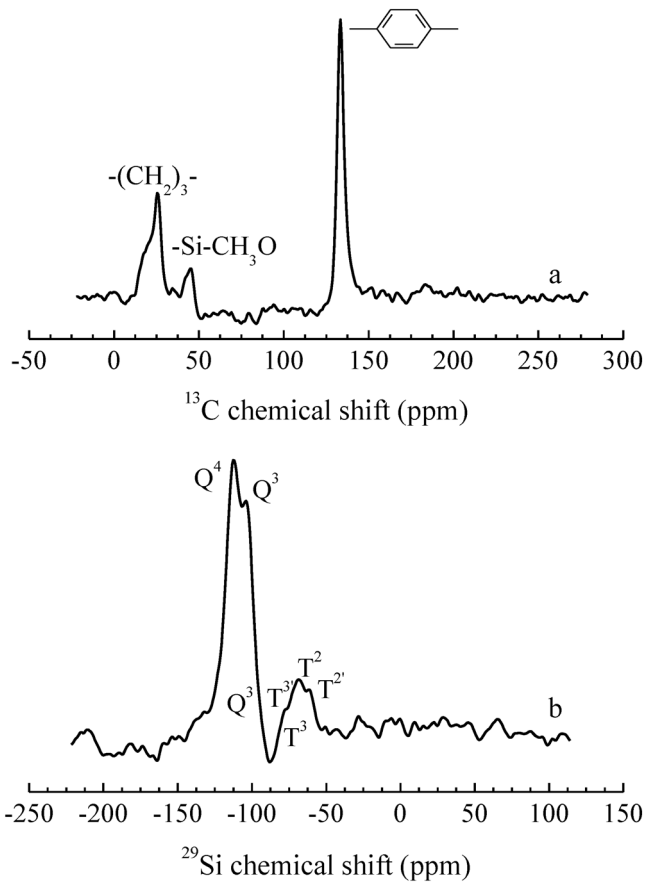

Fig. 5 ^{13}C (a) and ^{29}Si (b) MAS NMR spectra of Sn-Ph-PMOs-0.25 (T and T' refer to the Si species joint with phenylene group and **1**, respectively).

[22,24]. The signals at about 69.9 and 64 ppm can be assigned to T^2 species bridged by phenyl groups and that attached to **1**, respectively [27,29]. The presence of both Q^n and T^n species in the sample gives a convincing evidence for the incorporation of BTEB and **1** into the framework or silica wall.

Catalytic performance of organotin-functionalized Ph-PMOs in the synthesis of DMC from methanol and carbon dioxide

Figure 6 shows the DMC yield obtained over the Sn-Ph-PMOs-*x* samples at different reaction times. Clearly, the DMC yield increases with the reaction time for all the samples. The Sn-Ph-PMOs-*x* ($x > 0$) samples all give much higher activity than Sn-Ph-PMOs-0, as verified by the higher TON (turnover number, mole of DMC per mole of Sn) obtained on the former samples regardless of reaction time. The DMC yield increases with increasing the amount of bridging phenyl groups incorporated into the framework, although the degree of this increase is reduced gradually.

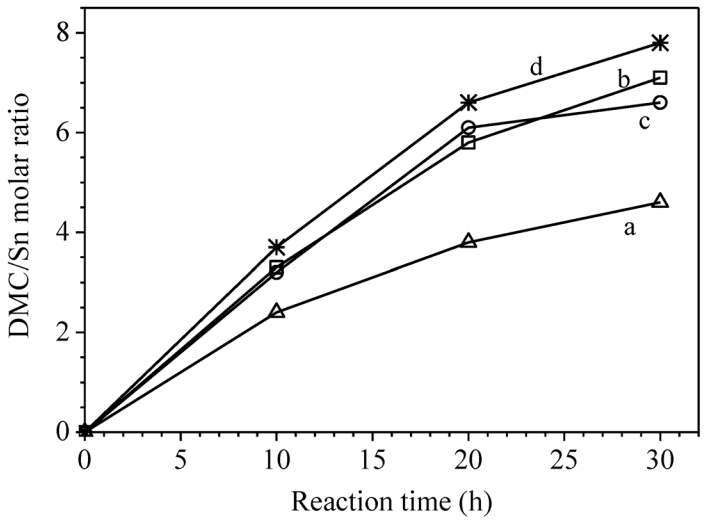

Fig. 6 Dependence of the DMC/Sn molar ratio obtained over (a) Sn-Ph-PMOs-0, (b) Sn-Ph-PMOs-0.25, (c) Sn-Ph-PMOs-0.67, and (d) Sn-Ph-PMOs-4.0 on the reaction time (reaction conditions: 0.05 g catalyst, 20 mL methanol, CO_2 pressure of 18.0 MPa, reaction temperature of 180 °C).

Direct synthesis of DMC from methanol and CO_2 is a thermodynamically restricted process, and the catalyst is easily deactivated by water formed during the reaction [30]. Thus, timely removal of water from the reaction system will considerably promote the formation of DMC [31]. Figure 7 shows the adsorption isotherms of H_2O on the Sn-Ph-PMOs-*x* samples at 25 °C. The uptake of H_2O decreases with increasing BTEB amount in the samples, showing an enhanced hydrophobicity. Thus, the thermodynamic balance would be broken in the local region around the active organotin sites, and the catalytic stability would be enhanced for the Sn-Ph-PMOs-*x* ($x > 0$) by repelling H_2O from the active sites, consequently, giving a higher DMC yield. The coordination states of Sn species in Sn-Ph-PMOs-*x* is different from that in Sn-Ph-PMOs-0, this may also contribute to the high activity of Sn-Ph-PMOs-*x*. It has been shown that the octahedral Sn species and tiny Sn oxide clusters may be more active than tetrahedral Sn species for the direct synthesis of DMC from methanol and CO_2 [24]. Sn-Ph-PMOs-*x* ($x > 0$) contains a large number of hexa-coordinated Sn species and/or tiny Sn oxide clusters (Fig. 4), while most of Sn species are tetrahedrally coordinated in Sn-Ph-PMOs-0. As a result, although Sn-Ph-PMOs-0.25 shows a similar H_2O adsorption capacity to Sn-Ph-PMOs-0, it exhibits a higher TON.

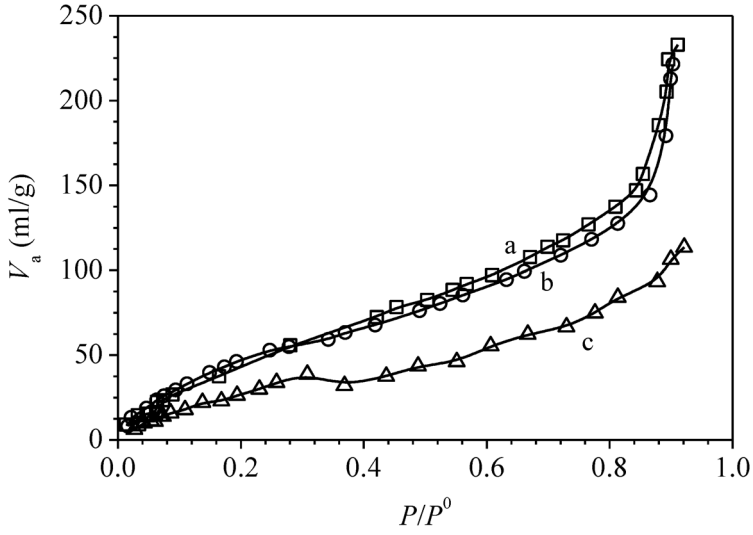

Fig. 7 Adsorption isotherms of H_2O on (a) Sn-Ph-PMOs-0, (b) Sn-Ph-PMOs-0.25, and (c) Sn-Ph-PMOs-4.0 at 25 °C.

Figure 8 shows that the DMC yield obtained over Sn-Ph-SBA-15-0.25 monotonically increases with increasing reaction temperature up to 200 °C within 10 h. Nevertheless, a further increase in the reaction temperature has no great effect on the DMC yield; this may be due to a partial degradation of **1** and/or a change in the coordination states of Sn species. As expected, the DMC yield obtained over Sn-Ph-PMOs-0.67 increases steadily with increasing CO_2 pressure (Fig. 9), because it favors the shift of the reaction toward the production of DMC and makes the reaction mixture more homogeneous by forming supercritical CO_2 medium at high pressure [32].

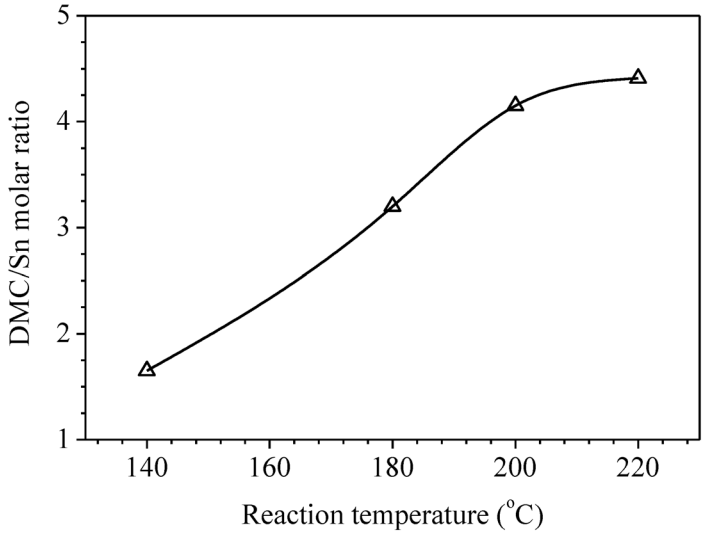

Fig. 8 Dependence of the DMC/Sn molar ratio obtained over Sn-Ph-PMOs-0.67 on the reaction temperature (reaction conditions: 0.05 g catalyst, 20 mL methanol, CO_2 pressure of 18.0 MPa, reaction time of 10 h).

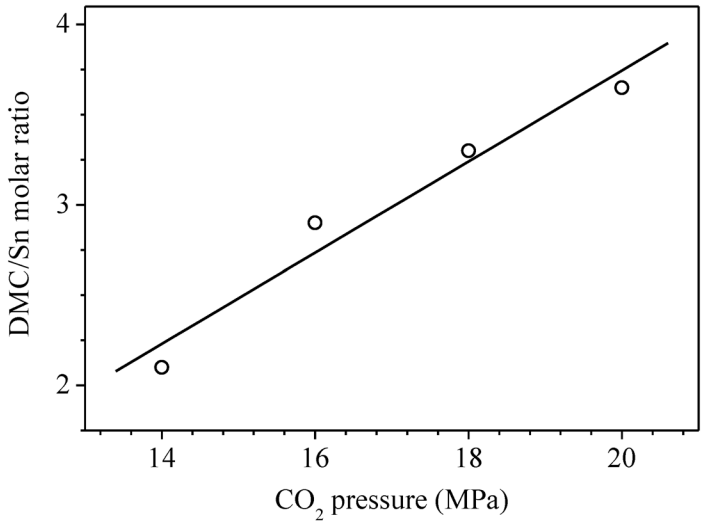

Fig. 9 Dependence of the DMC/Sn molar ratio obtained over Sn-Ph-PMOs-0.25 on the CO_2 pressure (reaction conditions: 0.05 g catalyst, 20 mL methanol, reaction temperature of 180 °C, reaction time of 10 h).

Figure 10 shows the catalytic results of Sn-Ph-PMOs-0.67 for the synthesis of DMC from methanol and CO_2 within five repeated runs with catalyst recycling. After each run, the catalyst was recovered by centrifuging, washing with methanol, and drying at 60 °C under vacuum conditions. The regenerated sample was then used for the next run under the same reaction conditions. It is clear that the DMC yield obtained is almost the same within five repeated runs; the DMC/Sn molar ratios are in the range of 3.0–3.4. This shows that Sn-Ph-PMOs-*x*, like the organotin-functionalized mesoporous silicas prepared by the co-condensation or the post-grafting method [22,29], is also highly stable in the reaction process of synthesis of DMC from methanol and CO_2.

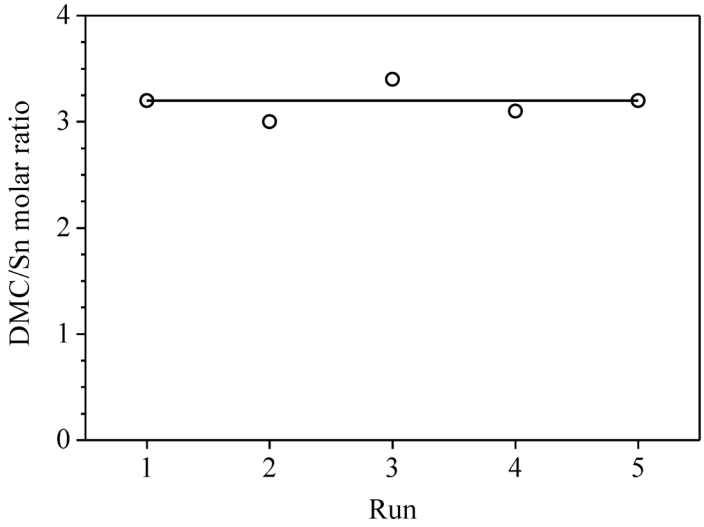

Fig. 10 DMC/Sn molar ratios obtained over Sn-Ph-PMOs-0.67 within five runs with catalyst recycling (reaction conditions: 0.05 g catalyst, 20 mL methanol, CO_2 pressure of 18.0 MPa, reaction temperature of 180 °C, reaction time of 10 h).

CONCLUSIONS

An organotin-functionalized mesoporous benzene-silica with high structure order has been prepared by in situ tethering/incorporating organotin compound on/into the pore wall during the synthesis of mesoporous benzene-silica. This material shows much higher activity than the organotin-functionalized mesoporous silicas prepared by the co-condensation and the grafting methods in the direct synthesis of DMC from methanol and CO_2 due to its enhanced surface hydrophocibity and the presence of a large number of hexa-coordinated Sn species and tiny Sn oxide clusters. The material also exhibits high catalytic stability upon reusage. The DMC yield increases substantially with increasing CO_2 pressure.

ACKNOWLEDGMENTS

The authors are grateful for the financial supports of the National Natural Science Foundation of China (20971095), the National Basic Program (2009CB226101), the Natural Science Foundation of Shanxi Province (2010011014-4), the Foundation for returned overseas scholars of Shanxi Province (2008-10), and the Knowledge Innovation Program of the Chinese Academy of Sciences (KJCX2.YW.H16).

REFERENCES

1. B. Hatton, K. Landskron, W. Whitnall, D. Perovic, G. A. Ozin. *Acc. Chem. Res.* **38**, 305 (2005).
2. G. Kickelbick. *Angew. Chem., Int. Ed.* **43**, 3102 (2004).
3. W. J. Hunks, G. A. Ozin. *J. Mater. Chem.* **15**, 3716 (2005).
4. T. Asefa, M. J. MacLachlan, H. Grondey, N. Combs, G. A. Ozin. *Angew. Chem., Int. Ed.* **39**, 1808 (2000).
5. S. Shylesh, R. K. Jha, A. P. Singh. *Microporous Mesoporous Mater.* **94**, 364 (2006).
6. B. A. Treuherz, Y. Z. Khimyak. *Microporous Mesoporous Mater.* **106**, 236 (2007).
7. S. Inagaki, S. Guan, T. Ohsuna, O. Tersaki. *Nature* **416**, 304 (2002).
8. W. J. Hunks, G. A. Ozin. *Chem. Mater.* **16**, 5465 (2004).
9. M. P. Kapoor, Q. H. Yang, S. Inagaki. *J. Am. Chem. Soc.* **124**, 15176 (2002).
10. A. Kuschel, S. Polarz. *Adv. Funct. Mater.* **18**, 1272 (2008).
11. G. Kickelbick. *Angew. Chem., Int. Ed*. **43**, 3102 (2004).
12. Q. H. Yang, J. Liu, L. Zhang, C. Li. *J. Mater. Chem.* **19**, 1945 (2009).
13. S. Shylesh, Ch. Srilakshmi, A. P. Singh, B. G. Anderson. *Microporous Mesoporous Mater.* **99**, 334 (2007).
14. S. Shylesh, A. P. Singh. *Microporous Mesoporous Mater.* **94**, 127 (2006).
15. M. Morishita, Y. Shiraishi, T. Hirai. *J. Phys. Chem. B* **110**, 127 (2006).
16. Q. H. Yang, J. Liu, J. Yang, M. P. Kpoor, S. Inagaki, C. Li. *J. Catal.* **228**, 265 (2004).
17. D. Coutinho, C. R. Xiong, K. J. Balkus Jr. *Microporous Mesoporous Mater.* **108**, 86 (2008).
18. D. M. Jiang, J. S. Gao, J. Yang, W. G. Su, Q. H. Yang, C. Li. *Chem. Mater.* **18**, 6012 (2006).
19. A. A. Shaikh, S. Sivaram. *Chem. Rev.* **96**, 951 (1996).
20. Y. Ono. *Appl. Catal. A* **155**, 133 (1997).
21. Y. Ono. *Pure Appl. Chem.* **68**, 367 (1996).
22. J. Kizlink, I. Pastucha. *Collect. Czech. Chem. Commun.* **60**, 687 (1995).
23. J. M. Batt. *Appl. Organometal. Chem.* **19**, 458 (2005).
24. B. B. Fan, J. L. Zhang, W. B. Fan, R. F. Li. *Catal. Lett.* **121**, 297 (2008).
25. J. Liu, Q. H. Yang, M. P. Kapoor, N. Steoyama, S. Inagaki, J. Yang, L. Zhang. *J. Phys. Chem. B* **109**, 12250 (2005).
26. K. Chaudhari, T. K. Das, P. R. Rajmohanan, K. Lazar, S. Sivasanker, A. J. Chandwadkar. *J. Catal.* **183**, 281 (1999).
27. Q. H. Yang, M. P. Kapoor, S. Inagaki. *J. Am. Chem. Soc*. **124**, 9694 (2002).

28. M. J. Jia, A. Seifert, M. Berger, H. Giegengack, S. Schulze, W. R. Thiel. *Chem. Mater.* **16**, 877 (2004).
29. B. B. Fan, H. Y. Li, W. B. Fan, J. L. Zhang, R. F. Li. *Appl. Catal., A* **372**, 94 (2010).
30. K. Almusaiteer. *Catal. Commun.* **10**, 1127 (2009).
31. T. Sakakura, J. C. Choi, Y. Satio, T. Sako. *Polyhedron* **19**, 573 (2000).
32. D. Ballivet-Tkatchenko, S. Chambrey, R. Keiski, R. Ligabue, L. Plasseraud, P. Richard, H. Turunen. *Catal. Today* **115**, 80 (2006).

